^{87}Sr Lattice Clock with Inaccuracy below 10^{-15}

Martin M. Boyd, Andrew D. Ludlow, Sebastian Blatt, Seth M. Foreman, Tetsuya Ido,* Tanya Zelevinsky, and Jun Ye

JILA, National Institute of Standards and Technology and University of Colorado, Department of Physics, University of Colorado, Boulder, Colorado 80309-0440, USA

(Received 7 November 2006; published 21 February 2007)

Aided by ultrahigh resolution spectroscopy, the overall systematic uncertainty of the $^1S_0$-$^3P_0$ clock resonance for lattice-confined ^{87}Sr has been characterized to 9×10^{-16}. This uncertainty is at a level similar to the Cs-fountain primary standard, while the potential stability for the lattice clocks exceeds that of Cs. The absolute frequency of the clock transition has been measured to be 429 228 004 229 874.0(1.1) Hz, where the 2.5×10^{-15} fractional uncertainty represents the most accurate measurement of a neutral-atom-based optical transition frequency to date.

DOI: 10.1103/PhysRevLett.98.083002 PACS numbers: 32.80.Qk, 42.62.Eh, 42.62.Fi

The significant advances in femtosecond comb technology [1–3] in the past decade have sparked immense interest in atomic clocks based on optical transitions [4]. These transitions have large line quality factors (Q) [5,6], which will provide orders of magnitude improvement in clock stability over state-of-the-art microwave clocks. An optical clock based on a single trapped Hg^+ ion has recently surpassed Cs-fountain clocks [7,8] in terms of accuracy, with clock systematics reduced to 7×10^{-17} [9]. Other high accuracy ion standards include Sr^+ [10,11] and Yb^+ [12]. The high line Q allows a stability comparable to the best achieved thus far with Cs, despite the fact that the single-ion signal-to-noise ratio (S/N) is drastically reduced compared to microwave systems, which typically employ $\sim 10^5$ atoms. Optical lattice clocks show promise for reaching a level of accuracy comparable to the ion systems, with significantly improved stability due to the large number of atoms involved in the measurement. This stability gain has spurred an intensive investigation of lattice clocks based on spin-forbidden transitions in alkaline-earth atoms, specifically in Sr [5,13–16] and Yb [17,18], where the trapping potential is designed to allow accurate measurements effectively free of both ac Stark shifts [13,19,20] and motional effects which can hamper optical clocks based on atoms in free space [21–23].

While the clock-stability benefits provided by the optical lattice method seem clear [5,18], reaching the accuracy level of the microwave standards remains a paramount issue in the field. Recently, great strides towards this goal have been taken, as a troublesome 4σ disagreement between the first two high accuracy experiments using ^{87}Sr [14,15] has been resolved by a third independent investigation [16] and a revised report by the authors of Ref. [14] published shortly thereafter [24]. Agreement between the three groups speaks strongly for the lattice clock as a future candidate for redefinition of the SI second; however, to be competitive with the current Cs-fountain clocks, the overall systematics must be reduced well below the 10^{-15} level.

In this Letter, we report a detailed study of the systematic uncertainty associated with the ^{87}Sr $^1S_0$-$^3P_0$ clock transition frequency at the level of 9×10^{-16}. This measurement, aided mainly by the record level line Q achieved recently [5], shows that the Sr lattice clock can reach an accuracy level competitive with Cs-fountains, while the potential stability for the system is far greater. An absolute frequency measurement of the transition is also reported with an uncertainty of 2.5×10^{-15}, limited by a Cs-calibrated NIST H-maser reference.

Full details of the cooling and trapping system used in this work are discussed elsewhere [15,25]. In brief, ^{87}Sr atoms are captured from a thermal beam into a magneto-optical trap (MOT) based on the $^1S_0$-$^1P_1$ cycling transition. Second stage cooling, using a dual frequency $^1S_0$-$^3P_1$ MOT [26], is performed concurrently with the loading of a vertical one-dimensional lattice, yielding $\sim 2 \times 10^4$ atoms at a temperature of 1.5 μK. The lattice is operated at the Stark cancellation wavelength [20] with an intensity $I_0 = 5$ kW/cm^2 (83% of which forms the standing wave due to window losses), resulting in measured longitudinal and radial trap frequencies of 40 kHz and 125 Hz, respectively. The atoms are distributed over ~ 80 lattice sites with a density $\rho_0 = 5 \times 10^{11}$ cm^{-3}. The spectroscopy sequence for the 1 mHz $^1S_0$-$^3P_0$ clock transition begins with a Rabi pulse from a highly frequency-stabilized diode laser [27] that is copropagated and copolarized with the lattice laser. With some atoms shelved in the $^3P_0$ state, the remaining $^1S_0$ population is heated out of the lattice by exciting the $^1S_0$-$^1P_1$ transition. The $^3P_0$ atoms are then driven back to the ground state, by pumping through intermediate states, and the population is measured by again driving the $^1S_0$-$^1P_1$ transition and detecting scattered photons. This process is repeated each time atoms are loaded into the lattice, as the laser frequency is tuned. The time window for the Rabi pulse is varied within 40–480 ms depending on the desired Fourier width (22–1.8 Hz). The time dedicated for cooling and state readout for each shot is ~ 900 ms.

The $^1S_0(F = 9/2)$-$^3P_0(F = 9/2)$ transition, facilitated by nuclear-spin-induced state mixing [28], suffers from a differential Landé g factor of the clock states, with the $^3P_0$ magnetic sensitivity being $\sim 60\%$ larger than that of the ground state. The resultant Zeeman shift

of $-109m_F$ Hz/G [5] (1 G $= 10^{-4}$ T, and m_F indexes the magnetic sublevel) can be a limitation in terms of the achievable accuracy and line Q in the presence of magnetic fields. Figure 1(a) shows a spectrum for an 80 ms probe time, representing the parameters typically used in the work reported here, yielding a FWHM (full width at half maximum) linewidth of 10.6(3) Hz. Given the line Q and typical S/N (~10), a clock instability of less than 3×10^{-15} at 1 s is expected. Reaching the atom-shot noise would further reduce the instability by a factor of 10. The narrowest resonances have so far been achieved when a resolved nuclear sublevel is used for spectroscopy as shown in Fig. 1(b). Here linewidth limitations from magnetic fields or state-dependent Stark shifts are eliminated, and widths below 2 Hz are repeatably observed.

As a general approach for evaluating systematics, an interleaved scheme is used where the parameter of interest is cycled through different values, synchronized with each frequency step of the probe laser across the resonance. The interleaved data are then separated into resonance profiles for each parameter value, allowing the center frequency (relative to the laser cavity), and hence the slope of the frequency shift, to be measured for a variety of parameters in a short time. This allows us to measure shifts against the probe laser, which has a stability superior to our available microwave reference [27].

Of the many effects to be characterized for an optical lattice clock, the effect of the lattice laser itself remains a focal point. The differential light shifts of the clock states due to the scalar, vector, and tensor polarizabilities all vary linearly with trap intensity and can be strongly suppressed with an appropriate choice of lattice wavelength [17,19]. Higher-order Stark shifts, due to the hyperpolarizability of the clock states, are negligibly small ($<10^{-17}$) [20] at our operating intensity and wavelength. Hence, a linear extrapolation to the zero-intensity

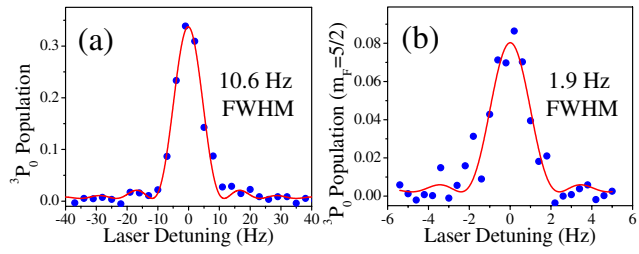

FIG. 1 (color online). High resolution spectroscopy of the $^1S_0$-$^3P_0$ transition. (a) A Fourier-limited resonance profile for typical experimental parameters. A sinc^2 fit is shown as a red curve, giving a linewidth (FWHM) of 10.6(3) Hz ($Q \simeq 4 \times 10^{13}$). (b) Spectroscopy of an isolated nuclear-spin component yields a linewidth of 1.9(2) Hz ($Q \simeq 2.3 \times 10^{14}$), consistent with the 1.8 Hz Fourier limit for the 0.48 s probe time. The spectra in both (a) and (b) are taken without averaging or normalization, and the vertical axes are scaled by the total number of atoms (2×10^4). The S/N in (a) is limited by shot to shot atom number fluctuation (10%), whereas the probe laser frequency noise is the dominant effect in (b) [5].

clock frequency is sufficient to characterize the total Stark shift from all contributors mentioned above. An example of this is shown in Fig. 2(a), where four different values of the lattice intensity are interleaved during a single trace taking less than 1 min. To reduce the shift uncertainty, 776 single measurements (using 2, 4, or 8 interleaved intensity values) were made, averaging to a Stark shift of $-108(257)\,\mathrm{mHz}/I_0$ for a wavelength $\lambda_0 = 813.4280(5)$ nm. The Gaussian-shaped histogram [Fig. 2(b)] summarizes the lattice Stark shift measurements.

The effect of atomic density on the transition frequency is explored in a similar fashion as densities ranging within $(0.2\text{–}1)\rho_0$ are interleaved (by varying the number of atoms in the MOT). A histogram of 422 measurements of the density effect is shown in Fig. 2(c), resulting in a shift coefficient of 3(140) mHz/ρ_0. Notably, the upper limit of the density-related fractional frequency shift of 5.6×10^{-28} cm^{-3} is ~10^6 times smaller than for Cs [7,8].

The ten nuclear-spin sublevels of the clock transition result in systematic effects related to magnetic and optical fields. For example, the asymmetric distribution of population among the sublevels can be a central systematic issue when using unpolarized atomic samples, as any m_F-dependent magnetic or optical interaction can cause a frequency shift, even if the sublevels are shifted symmetrically about the center. The differential g factor of the clock states provides the most significant effect as it leads to a sensitivity to magnetic fields of nearly 500 Hz/G for the stretched states. Three orthogonal sets of Helmholtz coils are used to characterize frequency shifts caused by the Zeeman sensitivity of the nuclear-spin sublevels. Figure 3 summarizes the characterization along one of these three axes. For each direction, the transition linewidth is used to find the field minimum as shown in Fig. 3(a). The narrow 10 Hz resonances allow the field zero to be constrained within 10 mG for each axis. Frequency shift sensitivity is explored using the interleaved scheme with the results for the featured axis shown

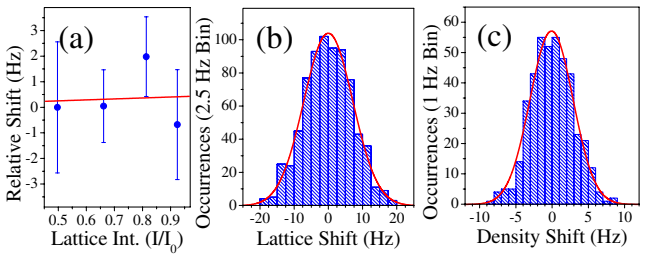

FIG. 2 (color online). (a) A single measurement of the lattice Stark shift achieved using four interleaved intensities during a scan of the clock transition. For this measurement, the shift is 0.4(4.4) Hz/I_0. (b) Histogram of 776 single measurements [such as in (a)] of the Stark shift for our typical intensity I_0. (c) Histogram of 422 measurements in which the atomic density is varied by a factor of 5 during spectroscopy. Gaussian fits (red curve) to the data in (b) and (c) are shown.

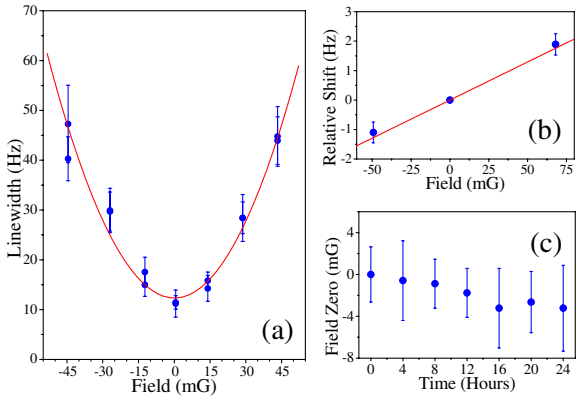

FIG. 3 (color online). Effect of a magnetic field on the transition linewidth and frequency. (a) The magnetic field is calibrated using the width of the narrow resonance. The data are fit to a parabola, determining the field zero within 4 mG. (b) The result of 112 interleaved measurements where the field is varied during spectroscopy. The frequencies of the zero field values are used as a reference for presentation purposes. The slope of all of the measurements for this axis yields an average value of 26(4) Hz/G. (c) Summary of field calibrations during the 24-hour absolute frequency measurement.

in Fig. 3(b). Here the average values for 112 measurements are shown, yielding a slope of 26(4) Hz/G. Similar measurements were performed for the other two axes, yielding 22(7) and 12(3) Hz/G, respectively. The fields for the three axes are zeroed below 5, 5, and 10 mG, respectively, resulting in a total Zeeman uncertainty of 5.3×10^{-16}. This gives insight into the minimal effect of the vector light shift which causes symmetric m_F-dependent shifts proportional to the degree of lattice ellipticity and trapping intensity [17,19]. The resultant splitting for the stretched states is estimated as less than 8 $(\mathrm{Hz/rad})/I_0$. To combat this effect, a high extinction polarizer ($>10^4$) is used for the lattice and probe beam, and while the vacuum chamber windows likely reduce the polarization purity, rotations of even a few degrees are equivalent to a sub-mG residual field, attesting to the insignificance of this effect compared to the differential g factor.

Systematics related to the probe laser were considered in two respects. First, the probe can cause Stark shifts of the clock states by coupling to external levels. Second, asymmetric motional sidebands could cause line pulling. This effect is minimal as the sidebands are well resolved (even the radial sidebands are detuned by more than 10 times the transition width) and are observed only for large probe intensities. These effects were checked experimentally by varying the probe power by more than an order of magnitude during 77 measurements. To eliminate Stark shifts from other sources, all lasers used for cooling, trapping, and detection are switched with both acousto-optic modulators and mechanical shutters. Shifts from blackbody radiation (BBR) are calculated [29] based on temperature measurements of the vacuum chamber and a nearby heated viewport during the experiment.

Table I summarizes the dominant systematic uncertainties for spectroscopy of the clock transition, reported in terms of fractional frequency. A total uncertainty of 0.88×10^{-15} is achieved, representing the first experimental verification that the lattice technique can reach inaccuracies below the 10^{-15} level, comparable with Cs-fountains. The largest uncertainties are limited by technical issues such as a small dynamic range on the lattice intensity and sensitivity to stray magnetic fields. The fiftyfold reduction of the systematic uncertainty from our previous work [15] is mainly due to the improved line Q and direct use of the stable optical reference. Future work using isolated spin states should allow dramatic reduction in the nuclear-spin-related shifts, while significant reductions in the lattice shift uncertainty can be achieved using a larger range of intensities. Spin polarizing the atoms can minimize collision shifts via Fermi suppression, when spin polarization is pure and all atoms are in a single motional state of the trap (possible but not yet achieved in a lattice clock). Even then, shifts associated with other interatomic interactions must be measured [30].

To measure the absolute frequency of the ${}^1S_0$-${}^3P_0$ transition, a Cs-fountain-calibrated H-maser is used to stabilize a radio frequency synthesizer located at NIST. The synthesizer modulates the amplitude of a 1320 nm laser, which is transferred to JILA via a ~4 km fiber link [31,32]. The modulation frequency of 950 MHz is compared to the repetition rate of a femtosecond frequency comb locked to the spectroscopy laser. The maser and transfer system provide a 1 s instability of 2.5×10^{-13}, and, for the work reported here, the maser is calibrated to 1.7×10^{-15}. Passive transfer using the fiber link has been found to introduce frequency offsets as large as 1×10^{-14}, specifically related to periodic stretching and compressing of the fiber length owing to daily temperature variations. To eliminate this effect, the fiber length is stabilized using a fiber stretcher controlled by comparison of the local microwave phase at NIST with that of modulated light reflected back from JILA. While in-loop measurements show that the frequency transfer is stabilized to a few parts in 10^{17}, we assign a conservative uncertainty of 1×10^{-16} to account for other potential errors [33]. The reference synthesizer for the transfer can also cause frequency errors [34] as drifts in the synthesizer's temperature result in fractional shifts at the level of 4×10^{-14} $(\mathrm{K/h})^{-1}$. For the measurements reported here, the synthesizer is placed

TABLE I. Strontium lattice spectroscopy error budget.

Contributor	Correction (10^{-15})	Uncertainty (10^{-15})
ac Stark (lattice)	0.25	0.60
ac Stark (probe)	−0.02	0.12
ac Stark (BBR)	5.44	0.16
Zeeman effect	0	0.53
Density shift	−0.01	0.33
Total	5.66	0.88

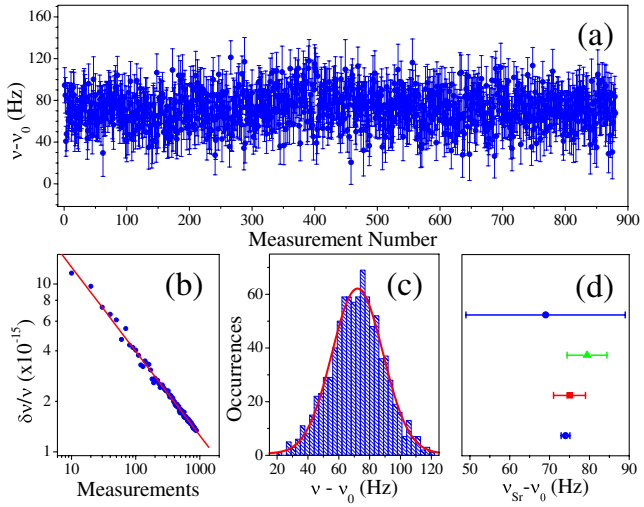

FIG. 4 (color online). Absolute frequency measurement of the $^1S_0$-$^3P_0$ transition. (a) Counting record of 880 measurements taken over a 24 h period yields a mean value of 71.8(6) Hz (corrected only for the maser offset in Table II). The offset frequency ν_0 is 429 228 004 229 800 Hz. (b) The uncertainty averages down as $N^{-0.501(4)}$, where N is the number of measurements (randomized), reaching 1.4×10^{-15}. (c) A histogram of the frequency measurements in (a) with a Gaussian fit (red curve) of the data. (d) Comparison of the final value ν_{Sr} reported here with recent measurements by the JILA (circle), SYRTE (triangle), and Tokyo (square) groups.

in a temperature-stabilized enclosure, and the temperature inside and outside the enclosure is monitored, resulting in a correction of $-1.7(7) \times 10^{-15}$.

A summary of 880 absolute frequency measurements spanning a 24 h period is shown in Fig. 4(a). Each point corresponds to a 30 s measurement of an 11 Hz spectrum with a frequency uncertainty of ~20 Hz, consistent with the Allan deviation of the H-maser. The data averages down with Gaussian statistics, as shown in Fig. 4(b) and in the histogram in Fig. 4(c). During the measurement, the Sr chamber temperature was continuously monitored, and the magnetic field was repeatedly calibrated [Fig. 3(c)] both by monitoring transition linewidths and by employing the zeroing technique in Fig. 3(a). Table II summarizes the relevant corrections and uncertainties associated with the absolute frequency measurement. The only significant corrections not determined by direct frequency measurements here are the BBR shift and the gravitational shift arising from the difference in elevation of the NIST Cs-fountain and the JILA Sr lattice. The frequency of the $^1S_0$-$^3P_0$ transition is 429 228 004 229 874.0(1.1) Hz, with the uncertainty mainly limited by the maser calibration. Figure 4(d) shows that this value agrees well with recent reports from the SYRTE [16] and Tokyo [24] groups as well as with our original value [15]. The final absolute frequency uncertainty of 2.5×10^{-15} corresponds to the most accurate optical frequency measurement for neutral atoms to date and falls short of only the recent Hg^+ ion result [9] as the most accurate optical measurement in any system.

TABLE II. Absolute frequency measurement error budget.

Contributor	Correction (10^{-15})	Uncertainty (10^{-15})
Sr syst. (Table I)	5.66	0.88
Maser calibration	−401.0	1.7
Synth. temp. drift	−1.7	0.7
Fiber transfer	0	0.1
Gravitational shift	1.25	0.02
Freq. meas. syst.	−395.8	2.0
Freq. meas. stat.	0	1.4
Total	−395.8	2.5
$\nu_{\mathrm{Sr}} - \nu_0$	74.0 Hz	1.1 Hz

We gratefully acknowledge technical contributions by S. Diddams and T. Parker on maser transfer. We also thank D. Hudson and M. Ting for help with the fiber link. This work was supported by ONR, NIST, and NSF.

*Present address: NICT, Tokyo, Japan.

[1] S. A. Diddams *et al.*, Phys. Rev. Lett. **84**, 5102 (2000).
[2] Th. Udem *et al.*, Nature (London) **416**, 233 (2002).
[3] S. T. Cundiff and J. Ye, Rev. Mod. Phys. **75**, 325 (2003).
[4] S. A. Diddams *et al.*, Science **306**, 1318 (2004).
[5] M. M. Boyd *et al.*, Science **314**, 1430 (2006).
[6] R. J. Rafac *et al.*, Phys. Rev. Lett. **85**, 2462 (2000).
[7] S. Bize *et al.*, J. Phys. B **38**, S449 (2005).
[8] T. P. Heavner *et al.*, Metrologia **42**, 411 (2005).
[9] W. H. Oskay *et al.*, Phys. Rev. Lett. **97**, 020801 (2006).
[10] H. S. Margolis *et al.*, Science **306**, 1355 (2004).
[11] P. Dubé *et al.*, Phys. Rev. Lett. **95**, 033001 (2005).
[12] T. Schneider *et al.*, Phys. Rev. Lett. **94**, 230801 (2005).
[13] H. Katori *et al.*, Phys. Rev. Lett. **91**, 173005 (2003).
[14] M. Takamoto *et al.*, Nature (London) **435**, 321 (2005).
[15] A. D. Ludlow *et al.*, Phys. Rev. Lett. **96**, 033003 (2006).
[16] R. Le Targat *et al.*, Phys. Rev. Lett. **97**, 130801 (2006).
[17] S. G. Porsev *et al.*, Phys. Rev. A **69**, 021403(R) (2004).
[18] Z. W. Barber *et al.*, Phys. Rev. Lett. **96**, 083002 (2006).
[19] V. Ovsiannikov *et al.*, Quantum Electron. **36**, 3 (2006).
[20] A. Brusch *et al.*, Phys. Rev. Lett. **96**, 103003 (2006).
[21] C. Degenhardt *et al.*, Phys. Rev. A **72**, 062111 (2005).
[22] G. Wilpers *et al.*, Appl. Phys. B **85**, 31 (2006).
[23] T. Ido *et al.*, Phys. Rev. Lett. **94**, 153001 (2005).
[24] M. Takamoto *et al.*, J. Phys. Soc. Jpn. **75**, 104302 (2006).
[25] T. H. Loftus *et al.*, Phys. Rev. A **70**, 063413 (2004).
[26] T. Mukaiyama *et al.*, Phys. Rev. Lett. **90**, 113002 (2003).
[27] A. D. Ludlow *et al.*, Opt. Lett. (to be published).
[28] H. J. Kluge and H. Sauter, Z. Phys. **270**, 295 (1974).
[29] S. G. Porsev and A. Derevianko, Phys. Rev. A **74**, 020502 (2006).
[30] D. E. Chang *et al.*, Phys. Rev. A **69**, 023810 (2004).
[31] J. Ye *et al.*, J. Opt. Soc. Am. B **20**, 1459 (2003).
[32] S. M. Foreman *et al.*, Rev. Sci. Instrum. (to be published).
[33] F. Narbonneau *et al.*, Rev. Sci. Instrum. **77**, 064701 (2006).
[34] J. E. Stalnaker *et al.*, in *Proceedings of the International Frequency Control Symposium, Miami, 2006* (IEEE, New York, 2006).